

A sensitive detection of high Rydberg atom with large dipole moment

Shan-Shan Zhang(张珊珊), Hong Cheng(成红), Pei-Pei Xin(辛培培), Han-Mu Wang(王汉睦), Zi-Shan Xu(徐子珊), Hong-Ping Liu(刘红平)

Citation: Chin. Phys. B . 2018, 27(7): 074207. **doi:** 10.1088/1674-1056/27/7/074207

Journal homepage: http://cpb.iphy.ac.cn; http://iopscience.iop.org/cpb

What follows is a list of articles you may be interested in

Coherently induced grating in refractive index enhanced medium

Zhuan-Zhuan Liu(刘撰撰), Yu-Yuan Chen(陈煜远), Jia-Yu Yuan(原佳宇), Ren-Gang Wan(万仁刚)

Chin. Phys. B . 2017, 26(12): 124209. **doi:** 10.1088/1674-1056/26/12/124209

High quality electromagnetically induced transparency spectroscopy of ^{87}Rb in a buffer gas cell with a magnetic field

Hong Cheng(成红), Han-Mu Wang(王汉睦), Shan-Shan Zhang(张珊珊), Pei-Pei Xin(辛培培), Jun Luo(罗军), Hong-Ping Liu(刘红平)

Chin. Phys. B . 2017, 26(7): 074204. **doi:** 10.1088/1674-1056/26/7/074204

Investigation of the nonlinear CPT spectrum of ^{87}Rb and its application for large dynamic magnetic measurement

Chi Xu(徐迟), Shi-Guang Wang(王时光), Yong Hu(胡勇), Yan-Ying Feng(冯焱颖), Li-Jun Wang(王力军)

Chin. Phys. B . 2017, 26(6): 064203. **doi:** 10.1088/1674-1056/26/6/064203

The effect of a permanent dipole moment on the polar molecule cavity quantum electrodynamics

Jing-Yun Zhao(赵晶云), Li-Guo Qin(秦立国), Xun-Ming Cai(蔡勋明), Qiang Lin(林强), Zhong-Yang Wang(王中阳)

Chin. Phys. B . 2016, 25(4): 044202. **doi:** 10.1088/1674-1056/25/4/044202

Electric dipole moments of lithium atoms in Rydberg states

Dong Hui-Jie, Huang Ke-Shu, Li Chang-Yong, Zhao Jian-Ming, Zhang Lin-Jie, Jia Suo-Tang

Chin. Phys. B . 2014, 23(9): 093202. **doi:** 10.1088/1674-1056/23/9/093202

A sensitive detection of high Rydberg atom with large dipole moment*

Shan-Shan Zhang(张珊珊)[1,2], Hong Cheng(成红)[1,2], Pei-Pei Xin(辛培培)[1,2], Han-Mu Wang(王汉睦)[1,2], Zi-Shan Xu(徐子珊)[1,2], and Hong-Ping Liu(刘红平)[1,2,†]

[1] *State Key Laboratory of Magnetic Resonance and Atomic and Molecular Physics, Wuhan Institute of Physics and Mathematics, Chinese Academy of Sciences, Wuhan* 430071, *China*
[2] *University of Chinese Academy of Sciences, Beijing* 100049, *China*

(Received 27 January 2018; revised manuscript received 16 April 2018; published online 25 June 2018)

We report a sensitive detection of high Rydberg atom with large dipole moment utilizing its deflection near a pair of parallel cylindrical copper rods which are oppositely charged. When the low-field seeking state Rydberg atoms fly across the gradient electric field formed by the pair of rods, they will be pushed away from the rods while the high-field seeking state ones will be attracted towards the rods. These atoms will form different patterns on an ion imaging system placed downwards at the end of the rods. The spatial distribution of the deflected atoms on the imaging system is also simulated, in good agreement with the experimental results, from which we can deduce the quantum state information of the excited atoms. This state resolvable Rydberg atom detection can be used for the dynamics research of the dipole–dipole interaction between atoms with large dipole moments.

Keywords: Rydberg Stark state, sodium atom, deflection, dipole moment

PACS: 42.50.Gy, 32.60.+i, 32.80.Qk, 32.70.Jz **DOI:** 10.1088/1674-1056/27/7/074207

1. Introduction

As an interesting and accessible system, Rydberg atoms in external fields have been an intensively studied subject in the physical realization of quantum simulation[1] and quantum information process.[2] Rydberg atoms with large electric dipole moments provide an opportunity for efficient control of their translational motion using inhomogeneous electric fields, leading to the experimental achievement of atomic guides,[3,4] mirrors,[5] lenses,[6] and traps.[7–9] In all processes, the quantum-state selection and detection of Rydberg atoms is essential to determine the population of prepared Rydberg states, which is required to read out the information of the quantum operations for quantum information processing.[1,2] The technique of the deflection of Rydberg atoms with a significant dipole moment in inhomogeneous electric fields proves an efficient way to selectively detect the internal states of neutral Rydberg atoms.[10,11]

The deflection of Rydberg atoms in inhomogeneous magnetic fields was first demonstrated in the classic Stern–Gerlach experiment in the 1920s.[12] In an external inhomogeneous electric field, the Rydberg atoms experience a force given by[13]

$$f(r) = -\mu \nabla F(r), \tag{1}$$

where F is the electric field, μ the electric dipole moment, and r the position of the particle. The force direction exerted on the Rydberg atom is dependent on the quantum state property. The change in kinetic energy of atoms under this force is positively relevant to the quantity of instantaneous induced dipole moment and determined by the integrated work exerted in the inhomogeneous electric field,[14,15] based on which we can deflect an atom with large dipole moment,[16] even in crossed fields.[17–19] For the atom beam naturally in gas phases at room temperature, for example, krypton atom beam, we can make the beam size very slim through alignment techniques such as narrowing the sizes of skimmers, and a clear deflected beam imaging can be observed.[16]

In this paper, we extend this technique to metal atoms, i.e., sodium, and demonstrate its applicability in a gradient electric field. This extending research is very important since metal atoms such as the sodium atom have a very low ionization potential energy, easily accessible to highly excited states through a one-photon excitation process and its spectroscopy in Rydberg states in electric fields has been extensively studied.[13,20–23]

2. Experimental setup

The experimental setup is based on the previous work,[24] and only the altered parts are detailed here. The kernel schematic diagram is shown in Fig. 1. A pulsed supersonic beam of ground-state sodium atoms is produced by expanding helium through a solenoid valve (General Valve, Series 9) in a vacuum, combined with the technique of laser-induced ablation. A rod of solid sodium rotates just aside the valve and ablated by focusing the fundamental output of a Nd:YAG laser (1064 nm, Continuum, Surelite I) on the surface of the metal rod. The generated atom vapor is blown away by the helium

*Project supported by the National Natural Science Foundation of China (Grant Nos. 91421305, 91121005, and 11674359) and the National Key Basic Research Program of China (Grant No. 2013CB922003).

†Corresponding author. E-mail: liuhongping@wipm.ac.cn

© 2018 Chinese Physical Society and IOP Publishing Ltd

jet expanded from the 0.4 mm skimmer into the second chamber. A repelling electric grid charged at 40 V is used to blow away the positive ions possibly generated by the ablation laser.

After being ejected into the second chamber, the atom beam is intersected by a UV laser beam at right angles in the region of a homogeneous field, where sodium atoms are excited from the ground state to a selected Rydberg state ($n = 20$–35) via a single-photon excitation process. The crossing point of the laser and atomic beam is located just in the middle of a pair of parallel Stark plates (10 mm × 10 mm) as shown in Fig. 1(a). The 244 nm UV radiation with linewidth of about 0.09 cm^{-1}, is produced by a barium borate (BBO) crystal through frequency-doubling the output of a tunable dye laser (Radiant Dyes laser, Narrow Scan) pumped by a Nd:YAG laser (Continuum Powerlite, Precision II, 8000 series).[24] The UV polarization is set to be parallel to the electric field to excite the $M_J = 0$ Stark Rydberg states.

The photoexcited Rydberg atoms continue their flying journey in an inhomogeneous field of paralleled copper cylindrical rods (length 70 mm, diameter 1.2 mm, center-to-center spacing 3.2 mm), located approximately 2 mm below the atomic beam. Rydberg atoms are deflected away or attracted towards the rods depending on whether they were excited to a low- or a high-field seeking Stark state. These trajectory-altered Rydberg atoms freely fly a distance of about 400 mm until arriving at an ionization region. In this field-free journey of flight, the atoms do not feel the deflecting force any longer but their space deflection perpendicular to the flight can be linearly magnified. After passing over the free flight region, the atomic beam enters the field-ionization region consisting of a fine-mesh grid and a pair of MCPs between which high voltage is applied to ionize the atoms. The MCPs are coupled to a P43 phosphor screen of fluorescence (lifetime ∼ 1.2 ms). The arrival of the ions can be imaged with a lens-coupled gated CCD camera (CoolSNAP HQ2, 8.98 × 6.71 mm^2) with spatial resolution 6.45 × 6.45 μm^2 pixels. The track history is diagramed in Fig. 1(b), where we can see the atoms starting at different incident parameters have different deflection angles, but all the deflections occur only close to the surface to the pair of rods.

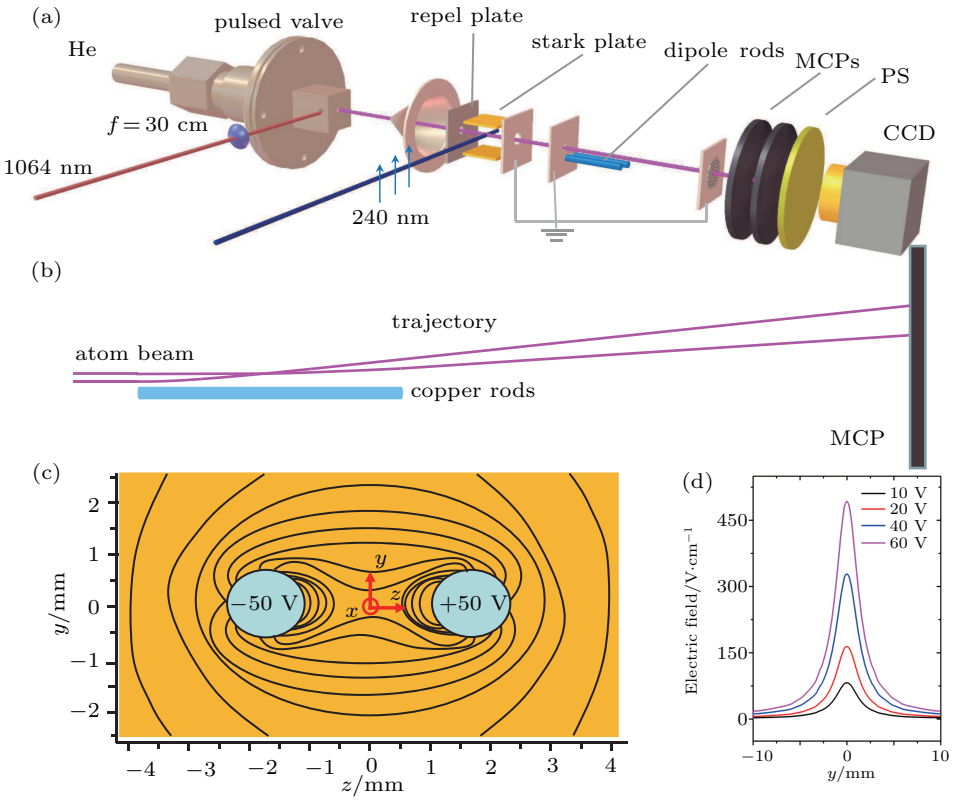


Fig. 1. (color online) Experimental setup for the deflection and detection of flying Rydberg sodium atoms. (a) The whole view of the experimental apparatus, (b) the schematic trajectories of atoms at two different incident parameters, (c) the electric field distribution formed by the charged pair of rods, and (d) the electric field along the y direction at $z = 0$ with charged voltage ±10 V (black line), ±20 V (red line), ±40 V (blue line), and ±60 V (pink line), respectively. The pair of Stark plates in panel (a) is used to selectively excite red and blue state Rydberg atoms through one-photon irradiation.

Specially, the electric field induced by the electrodes at opposite charge voltage $V = \pm 50$ V is simulated in a plane perpendicular to the rods and schematically shown in Fig. 1(c) with an electric field distribution along the y direction shown in Fig. 1(d) at charge voltages varying from ±10 V (black line), ±20 V (red line), ±40 V (blue line) to ±60 V (pink line), respectively. All distributions share the same profile and can be described by the same Lorentzian function but with differ-

ent amplitudes. The surfaces of electrodes facing the gas flow have been carefully polished to avoid spurious stray electric fields and sparking.

3. Results and discussion

To investigate the motion of Rydberg atoms in an inhomogeneous radial electric field surrounding a pair of copper rods, we select two states of large dipole moments but with opposite signs, i.e., 25p and 25s states belonging to the low- and high-field seeking states, respectively. The Stark maps and their dipole moments μ_d are shown in Figs. 2(a) and 2(b), both of which are calculated by the so-called exact quantum defect theory method extensively developed recently by our group.[25,26] According to the selection rules for electric dipole transitions in the absence of external electric fields, the 25s state cannot be populated by resonant single-photon excitation and we have to apply a weak electric field to mix the 25p state with the 25s one to make the transition enabled.

In Fig. 2(a), we can see that the 25s state undergoes a quadratic Stark shift (solid red lines) at low fields and its energy level deviates greatly due to a large quantum defect value for ns channel $\delta_s = 1.35$.[22,23] A similar behavior happens to the state 25p (solid blue lines) as well but with less deviation for a smaller quantum defect, $\delta_p = 0.85$.[22,23] Their corresponding electric dipole moments are calculated as shown in Fig. 2(b) and show opposite signs, but above the Inglis–Teller limit, the energy levels and the dipole moments are oscillating as a function of the electric field.

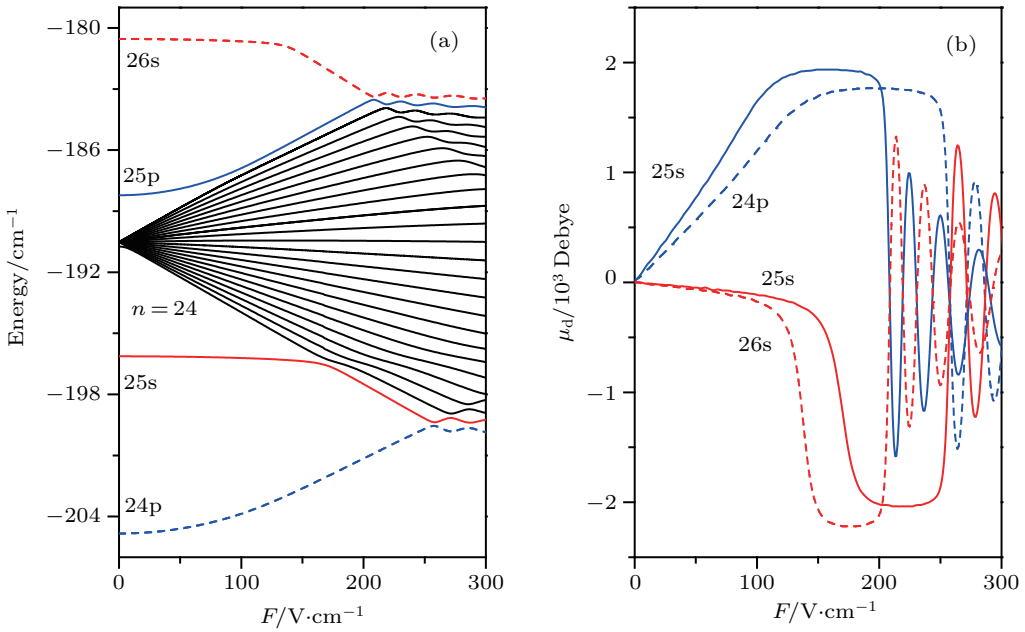


Fig. 2. (color online) Calculated Stark map for $n = 24$ manifold of sodium (a) and its corresponding dipole moments (b). The 25p and 25s states we are interested in are drawn in thick blue and red solid lines.

The force exerted on Rydberg–Stark atoms is proportional to the multiplication of the dipole moment and the gradient electric field. Compared with the 25p state, the 25s one is deflected towards the high-field region because the energy decreases with electric field strength. The 25s state (red lines in Fig. 2(b)) possesses a small induced dipole moment at the field below around 150 V/cm while the 25p state shows a large sharp slope around 150 V/cm below the Inglis–Teller limit. Above this value, the induced dipole moments oscillate for both 25s and 25p states, making little contribution for the deflection force.

We firstly excite the atom onto the Rydberg state 25p and study its kinetic behavior in the gradient electric field. The experimental result and theoretical simulation are shown in Figs. 3(a) and 3(b), respectively. We can notice a significant deflection for sodium atoms in 25p state and the deflection also varies with the strength of the applied electric field. As the 25p state is a low-field seeking state, it is deflected towards the low-field region, away from the rod pair. Since the dipole moment is a function of the applied electric field as shown in Fig. 2, we should carefully optimize the electric field applied on the Rydberg atoms. The simulation shown in Fig. 3(b) has employed a methodology described in Ref. [11] and the Stark map shown in Fig. 2, which is in good agreement with the experimentally observed images. In the simulation, we suppose the atomic motion is confined within the two-dimensional x–y plane at $z = 0$ and the rods are long enough. The Hamilton equations of motion for atomic center of mass coordinates then become

$$\frac{\partial x}{\partial t} = p_x/m, \tag{2a}$$

$$\frac{\partial p_x}{\partial t} = 0, \tag{2b}$$

$$\frac{\partial y}{\partial t} = p_y/m, \tag{2c}$$

$$\frac{\partial p_y}{\partial t} = -\mu_{\rm d}\frac{\partial F_y}{\partial y}, \tag{2d}$$

where $\mu_{\rm d}$ and F_y are functions of y, and their numerical values are taken from Figs. 2(b) and 1(b), respectively. A B-spline interpolation technique is used to valuate $\mu_{\rm d}$ and F_y at arbitrary internal coordinate (x,y) when numerically solving the time-dependent equation above. The initial velocity along the x-axis is Gaussian-sampled at $v = 1700 \pm 200$ m/s while the initial positions of atoms along the y-axis are also sampled following a Gaussian distribution. To mimic the atomic density in the z-direction shown in Fig. 1(b), a Gaussian distribution centered at $z = 0$ has been employed. The broadening technique in z and the atomic motion dominated by Eq. (2) give images shown in Fig. 3(b). The image detected on the CCD has been magnified by the field-free flight discussed previously and the optical system but both of them are linearly scaled in the y-direction. If not specified, arbitrary units are used in the image simulation as shown in Fig. 3.

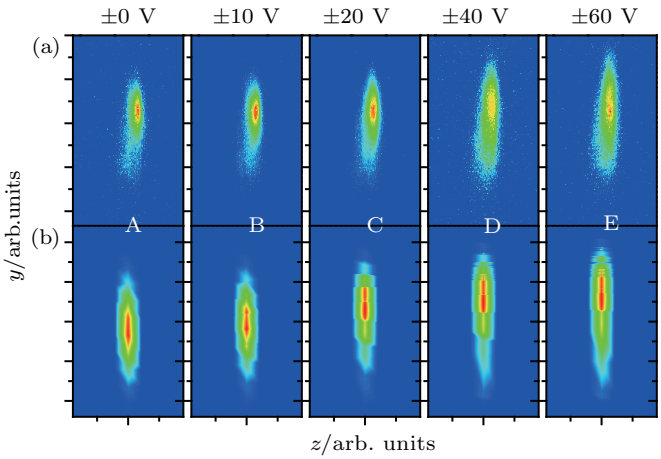


Fig. 3. (color online) Experimental (a) and simulated (b) deflection images of Rydberg atom in 25p state in inhomogeneous electric fields with different charge voltages ±0 V, ±10 V, ±20 V, ±40 V, and ±60 V.

Different from the mediocre deflection for the 25p state away from the rods, the deflection for the 25s state is towards the center line of the rod pair for an attraction force and shows a strong clipping effect for the image. The atomic image at zero deflection electric field is shown in Fig. 4(a) as a reference and its integrated signal along z is shown in Fig. 4(c). Once we apply a deflecting voltage on the rod pair, for example, applying ±45 V on the pair of copper rods, we can observe an image shown in Fig. 4(b), with its integrated one in Fig. 4(d). We can see that some atoms have been deflected away from the center and populated on one shoulder of the Gaussian distribution, which is greatly different from that for the 25p state. This is due to the inhomogeneous scattering by the gradient field for atoms of different initial incident positions in the y-direction, which will be discussed later.

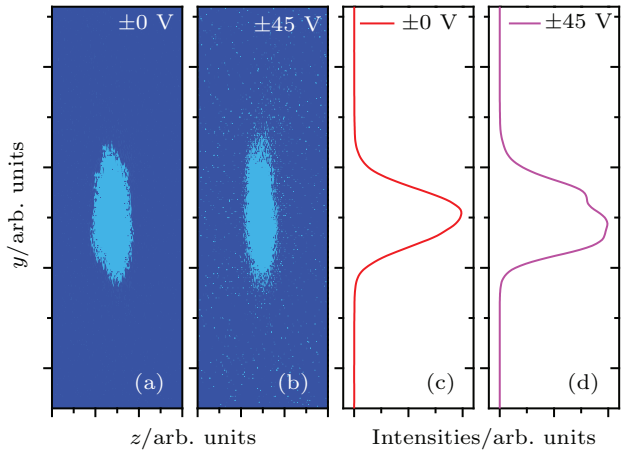


Fig. 4. (color online) Experimentally observed images of atomic cloud in zero field (a) and at copper rod voltage ±45 V (b). The corresponding distributions of the atomic cloud integrated along the z-direction are also shown in panels (c) and (d) for clearly viewing the clipping effect. The image size is displayed in arbitrary units since it is proportionally scaled by the optical imaging system.

This clipping effect on the image for the 25s state is dependent on the applied voltages on the rods. The integrated signals along y from experiment and simulation are shown in Figs. 5(a)–5(c) and Figs. 5(d)–5(f), respectively. The corresponding voltage takes values $V = 0$, $V = 45$ V, and $V = 55$ V. Here each simulated image is constructed from more than 100 thousands of trajectories sampling over the whole space of initial velocities and positions. All simulations are in good agreement with the experimental observations. Similar to the results shown in Fig. 4(d) at $V = 45$ V, the images at higher voltage $V = 55$ V also show an image clipping effect.

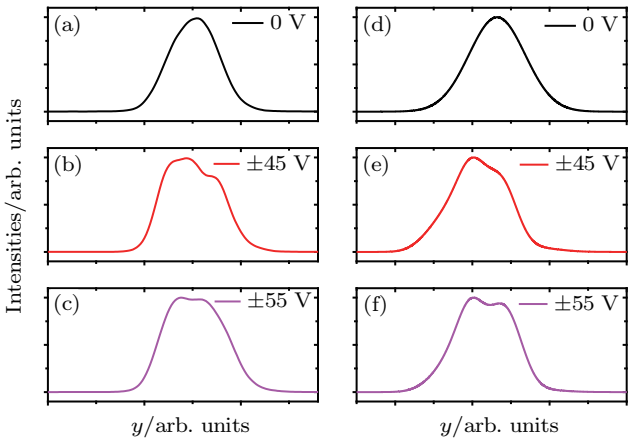


Fig. 5. (color online) The integrated image profiles from CCD-camera in panels (a)–(c) and their simulations in panels (d)–(f) for sodium atoms in 25s state in inhomogeneous electric field produced by the pair of copper rods, with applied voltage potentials 0 V, ±45 V, and ±55 V, respectively. Arbitrary units have been used as the same claim in Figs. 4(c) and 4(d).

The mediocre deflection for the 25p state away from the rods and the deflection for the 25s state with the clipping effect can be well explained by the atomic dipolar interaction with the applied gradient field. A simulation of the atomic dynamic kinetic movement close to the rods in real size scale is shown

in Fig. 6. The classical dynamics is described by the Hamilton equations in Eq. (2). We can see that the atomic trajectory varies for different initial positions along the y-direction for atoms on state either 25p (Fig. 6(a)) or 25s (Fig. 6(b)). For example, for the atom in the 25p state shown in Fig. 6(a), the trajectory denoted by D at $y(t=0)=1.5$ mm has the largest deflection angle. For the atoms with farther incident distance $y(t=0)>1.5$ mm, the deflection angle decreases slowly as depicted by E and F, while the atoms with shorter incident parameters such as C, B, and A nearly keep a straight flight.

For atoms in state 25s, this deflection is more sensitive to the initial incident distance $y(t=0)$ as shown in Fig. 6(b). Only for the atoms starting very close to the point D ($y(t=0)=1.6$ mm), the trajectories have great deflection angles thus resulting in a blowout of atom from the Gaussian distribution background, which provides a mechanism to selectively study the atoms at point D *in situ*. This sensitive detection method relies on the fact that the force exerted on Rydberg atoms by inhomogeneous electric fields is determined by the product of the electric field gradients and the induced dipole moment, and that the Rydberg atom experiences a huge deflection in the position only when it owns large induced dipole moments and large gradient values of electric fields, both of which are functions of the position coordinate y. This unique property can provide a mechanism for selecting a specific atom group in space with high resolution.

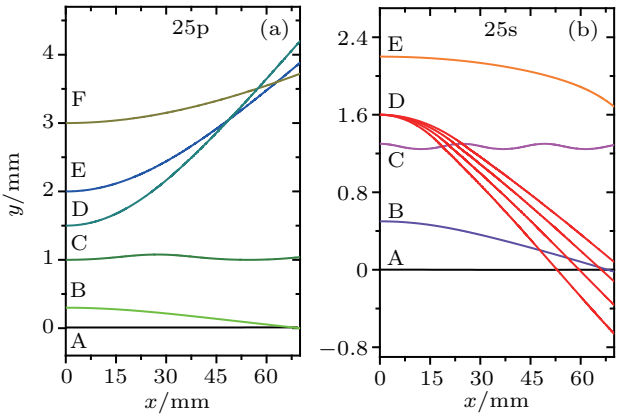


Fig. 6. (color online) Trajectory simulations for sodium atoms in 25p state (a) and in 25s state (b) at the rod pair of applied potential ±50 V. (a) Trajectories that have large deflections as denoted by D, E, and F, and possess small alterations labeled by A, B, and C. (b) The atoms are deflected only a little at A, B, C, and E, but a lot at D, showing a deflection property sensitive to the initial position along y.

In an ideal case, we can narrow the beam size to the μm scale, i.e., 100 μm, and observe only the Rydberg atoms starting at an exactly given $y(t=0)$ point. Therefore, the deflection of atom can be clearly seen on the image without background disturbing. However, for metal atoms, we cannot do this by narrowing the beam diameter to this size as the metal atom will deposit on the skimmer pin hole of small size and block it. This is different from the previous work for Kr,[16] where Kr is naturally in gas state and an application of small size pin hole is possible. As a result, our recorded image has a Gaussian background formed by the mediocre atoms which are not deflected at all or only a little deflected for the large beam size used. Even so, however, the unique scattering feature of atom in state 25s can avoid this disadvantage caused by the usage of metal atoms since its deflection trajectory is extremely sensitive to the initial position perpendicular to the beam, namely, $y(t=0)$, at the starting moment.

During the flight journey, it is possible for Rydberg atoms to get ionized due to the dipole-dipole interaction between them, but all ions generated in the collision are blown away perpendicularly by the applied field and invisible for the image detection system.

4. Conclusion

In summary, we demonstrate the deflection of a metal atom, i.e., sodium, on the Rydberg state in a gradient electric field formed by a pair of parallel cylindrical copper rods. In the experiment, the Rydberg sodium atoms are prepared onto the red/blue state in appropriate Stark fields, typically possessing the large induced dipole moments we are interested in. Particularly, the red state atom belonging to the high-field seeking state is attracted towards the dipole rods while the blue state atom belonging to the low-field seeking state is deflected away. In more detail, the force exerted on an atom is positively determined by the multiplication of the instantaneous induced dipole moment and the gradient of the electric field, thus providing a state sensitive detection of the Rydberg atom. The pair of rods can be geometrically designed to a small size and the maximum deflection occurs only in a very narrow space along the gradient direction, thus it can also be taken as a detector to monitor the specific group of an atom *in situ*, especially for metal atoms.

References

[1] Weimer H, Muller M, Lesanovsky I, Zoller P and Buchler H P 2010 *Nat. Phys.* **6** 382
[2] Saffman M, Walker T G and Molmer K 2010 *Rev. Mod. Phys.* **82** 2313
[3] Ko H and Hogan S D 2014 *Phys. Rev. A* **89** 053410
[4] Lancuba P and Hogan S D 2013 *Phys. Rev. A* **88** 043427
[5] Vliegen E and Merkt F 2006 *Phys. Rev. Lett.* **97** 033002
[6] Vliegen E, Limacher P A and Merkt F 2006 *Eur. Phys. J. D* **40** 73
[7] Hogan S D and Merkt F 2008 *Phys. Rev. Lett.* **100** 043001
[8] Seiler C, Hogan S D, Schmutz H, Agner J A and Merkt F 2011 *Phys. Rev. Lett.* **106** 073003
[9] Hogan S D, Seiler C and Merkt F 2013 *J. Phys. B: At. Mol. Opt. Phys.* **46** 045303
[10] Wall T E, Alonso A M, Cooper B S, Deller A, Hogan S D and Cassidy D B 2015 *Phys. Rev. Lett.* **114** 173001

[11] Goodgame A L and Softley T P 1999 *J. Phys. B: At. Mol. Opt. Phys.* **32** 4839
[12] Gerlach W and Stern O 1921 *Z. Phys.* **8** 110
[13] Gallagher T F 1994 *Rydberg Atoms* (Cambridge: Cambridge University Press)
[14] Vliegen E and Merkt F 2005 *J. Phys. B: At. Mol. Opt. Phys.* **38** 1623
[15] Vliegen E, Worner H J, Softley T P and Merkt F 2004 *Phys. Rev. Lett.* **92** 033005
[16] Townsend D, Goodgame A L, Procter S R, Mackenzie S R and Softley T P 2001 *J. Phys. B: At. Mol. Opt. Phys.* **34** 439
[17] Raithel G and Fauth M 1995 *J. Phys. B: At. Mol. Opt. Phys.* **28** 1687
[18] Raithel G, Fauth M and Walther H 1993 *Phys. Rev. A* **47** 419
[19] Raithel G, Held H, Marmet L and Walther H 1994 *J. Phys. B: At. Mol. Opt. Phys.* **27** 2849
[20] Pisharody S N, Zeibel J G and Jones R R 2000 *Phys. Rev. A* **61** 063405.
[21] Miculis K, Beterov I I, Bezuglov N N, Ryabtsev I I, Tretyakov D B, Ekers A and Klucharev A N 2005 *J. Phys. B: At. Mol. Opt. Phys.* **38** 1811
[22] Littman M, Zimmerman M, Ducas T, Freeman R and Kleppner D 1976 *Phys. Rev. Lett.* **36** 788
[23] Zimmerman M L, Littman M G, Kash M M and Kleppner D 1979 *Phys. Rev. A* **20** 2251
[24] Gao W, Yang H F, Cheng H, Zhang S S, Liu D F and Liu H P 2015 *Chin. Phys. B* **24** 013202
[25] Yang H F, Gao W, Quan W, Liu X J and Liu H P 2012 *Phys. Rev. A* **85** 032508
[26] Gao W, Yang H F, Cheng H, Liu X J and Liu H P 2012 *Phys. Rev. A* **86** 012517